THE SYNTHESIS AND TURNOVER

OF RAT LIVER PEROXISOMES

V. Intracellular Pathway of Catalase Synthesis

PAUL B. LAZAROW and CHRISTIAN de DUVE

From The Rockefeller University, New York 10021. Dr. Lazarow's present address is Department of Biological Sciences, Stanford University, Stanford, California 94305.

ABSTRACT

The subcellular distribution of the biosynthetic intermediates of catalase was studied in the livers of rats receiving a mixture of [³H]leucine and [¹⁴C]δ-aminolevulinic acid by intraportal injection. Postnuclear supernates were fractionated by a one-step gradient centrifugation technique that separates the main subcellular organelles, partly on the basis of size, and partly on the basis of density. Labeled catalase and its biosynthetic intermediates were separated from the gradient fractions by immunoprecipitation, and the distributions of radioactivity were compared with those of marker enzymes. The results show that catalase protein is synthesized outside the peroxisomes, but rapidly appears in these particles, mostly still in the form of the first hemeless biosynthetic intermediate. Addition of heme and completion of the catalase molecule take place within the peroxisomes. During the first 15 min after [³H]leucine administration, more than half of the newly formed first intermediate was recovered in the supernatant fraction, where it was found to exist as an aposubunit of about 60,000 molecular weight.

INTRODUCTION

It has been shown in the preceding paper of this series (22) that rat liver catalase is synthesized by way of two distinct intermediates, one without heme and having a turnover time of about 49 min, the other containing heme and having a turnover time of about 17 min. The topology of this process has been investigated in the present experiments. To this end, rats were killed at various times after the intraportal injection of a mixture of [³H]leucine and [¹⁴C]δ-aminolevulinic acid (ALA),[1] their livers were homogenized and

fractionated by a single-step density gradient centrifugation technique specially designed to provide optimal analytical resolution of the main subcellular organelles, and the distribution of the radioactivity that could be recovered by precipitation with anticatalase, without and after partial purification of catalase, was determined and compared with those of marker enzymes. The results presented here form part of the Ph.D. thesis of one of us (Lazarow [21]) and have been reported in a preliminary communication (20).

MATERIALS AND METHODS

Experimental Design

Rats were given [³H]leucine, alone or in combination with [¹⁴C]ALA, by intraportal injection, as de-

---

[1] *Abbreviations used in this paper:* ALA, δ-aminolevulinic acid; DAB, 3,3'-diaminobenzidine; ER, endoplasmic reticulum; PCI, purified catalase immunoprecipitate; PNS, postnuclear supernate; TCA, trichloroacetic acid; WFI, whole fraction immunoprecipitate.

scribed in the preceding paper (22). The animals were sacrificed at various times thereafter and their livers rapidly removed and chilled.

Homogenization of the livers in 0.25 M sucrose containing 0.1% ethanol was combined with the separation of a nuclear fraction as described by de Duve et al. (10), but using conditions such that the resulting postnuclear supernate (PNS) contained the equivalent of 0.2 g of liver/ml. The PNS was fractionated as described below, and the fractions, as well as the original PNS, were assayed for protein, RNA, marker enzymes, TCA-precipitable radioactivity, and immunoprecipitable radioactivity. Immunoprecipitation was carried out exactly as described in the preceding paper (22), both on the whole fractions to yield *whole fraction immunoprecipitates* (WFI), and after partial purification of catalase to yield *purified catalase immunoprecipitates* (PCI). Only goat globulins were used. The ^3H and ^{14}C content of the precipitates was determined by differential scintillation counting. The results were calculated and plotted in histogram form, according to Leighton et al. (24). All assays were performed also on the PNS and on the nuclear fractions. Thus total distributions, as well as recoveries, could be calculated.

Biochemical Assays

Catalase, protein, cytochrome oxidase, L-α-hydroxyacid oxidase, acid phosphatase, and glucose-6-phosphatase were assayed by the automated methods described by Leighton et al. (24). In some cases, catalase was measured by the hand method of Baudhuin et al. (2). RNA was determined as described by Blobel and Potter (4). Esterase was measured by a method developed in our laboratory by M. Baggiolini. In this assay, 0.1 ml of suitably diluted enzyme is mixed with 1 ml of 0.4 mM α-naphthyl acetate (Koch-Light Laboratories Ltd., Colnbrook, Buckinghamshire, England) in 50 mM phosphate buffer, pH 6.8, and incubated for 6 min at 25°C. Addition of 1 ml of ice-cold 1.0 M citrate buffer, pH 4.0, containing 5 μl of diazotized aniline yellow dye (44) serves both to stop the reaction and to couple the liberated α-naphthol. The optical density is read at 487 nm 10 min later. Activity is expressed in micromoles of substrate hydrolyzed per minute.

One-Step Gradient Fractionation Technique

The automatic Beaufay rotor was used in the manner described by Leighton et al. (24). 8 ml of PNS (1.6 g liver) were layered over a 26 ml aqueous sucrose gradient extending linearly with respect to volume between densities 1.10 and 1.27, itself resting on a 6 ml cushion of a sucrose solution of density 1.32. The gradient solutions were prepared by dissolving sucrose in water containing 5% (wt/wt) dextran-10

(believed to protect the peroxisomes [24]) and 0.1% ethanol (to protect the catalase [6]); they were buffered at pH 7.0 with 1 mM imidazole. Centrifugation was performed under control of the Integrator Accessory (Beckman Instruments, Inc., Spinco Div., Palo Alto, Calif.), in such a way as to achieve a value of 1.4×10^{10} s^{-1} for W, the time integral of the squared angular velocity (see Eq. 1).

These centrifugation conditions were chosen so as to be just sufficient to bring the peroxisomes near their equilibrium position in the lower part of the gradient, leaving the more slowly sedimenting microsomes still some distance away from their own isopycnic position. It was reasoned that in this manner an optimal separation would be achieved between the peroxisomes and the microsomes, including the dense RNA-rich vesicles of rough-surfaced endoplasmic reticulum (ER) which, at density equilibrium, overlap with the peroxisomes (1, 45). The required value of W was determined by computer simulation (Fig. 1).

For the purpose of these calculations, the integrated Svedberg equation for a spherical particle was rewritten as:

$$W = \int_{t_0}^{t} \omega^2 dt = \frac{9}{2r^2} \int_{x_0}^{x} \frac{\eta dx}{(\rho_p - \rho_m)x} = \frac{9}{2r^2} G(x), \quad (1)$$

and appropriate functions were computed to express the dependence on the radial distance x of the density ρ_m and viscosity η (9) of the medium (at 5°C), and of the particle density ρ_p, which is known to be a linear function of ρ_m (3). The assumption was made that all peroxisomes have an equilibrium density of 1.23 in aqueous sucrose. The equations used are given in the legend to Fig. 1. They allowed calculation of the integral $G(x)$, and thereby the radii r of the peroxisomes at different positions in the rotor for given values of W:

$$r = \sqrt{\frac{9G(x)}{2W}}. \quad (2)$$

The corresponding distribution of catalase was obtained from the measurements of Poole et al. (30). Their data, replotted cumulatively, were fitted mathematically as illustrated in Fig. 2.

As shown in Fig. 1, our calculations lead to the prediction that most of the peroxisomes should reach their equilibrium density when $W = 1.2\text{-}1.8 \times 10^{10}$ s^{-1}. In Fig. 3 are shown the results of an experiment performed with $W = 1.4 \times 10^{10}$ s^{-1}. Catalase and L-α-hydroxyacid oxidase show identical distributions, with about 30% of the activities remaining in the sample layer, and the remainder distributed around a density of 1.23 in a manner very similar to that reported by Leighton et al. (24) for the equilibrium distribution of peroxisomes. The observed
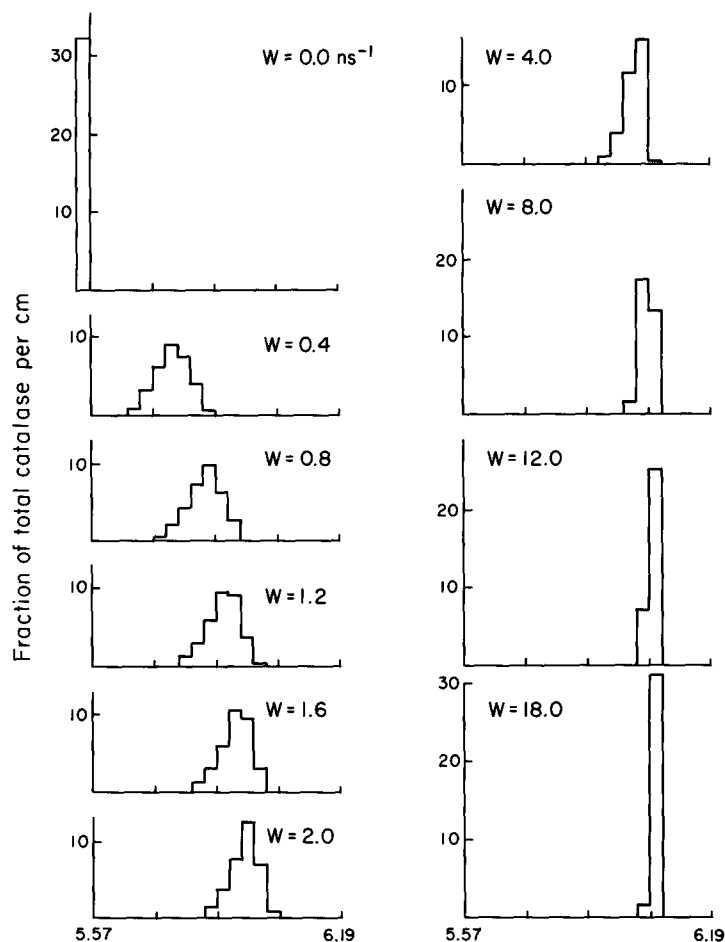
FIGURE 1 Computer simulation of peroxisome sedimentation through a sucrose gradient in the Beaufay rotor under conditions described in the text (radial limits of the gradient itself = 5.57 and 6.19 cm). $G(x)$ in Eq. 1 was computed from the following functions:

$$\rho_m(x) = 1.10 + \frac{x - 5.57}{6.19 - 5.57} \, (1.27 - 1.10), \tag{3}$$

$$\log_e \eta(x, 5°C) = \sum_{i=1}^{9} C_i \left[\rho_m(x) \right]^{(i-1)}, \tag{4}$$

in which constants C_1 to C_9 are: -7.985, 14.47, -6.711, -4.827, 1.825, 10.06, -4.980, -5.196, 3.728. η is expressed here in centipoises (it is in poises in Eq. 1).

$$\rho_p(x) = \frac{1.23 + 2.55 \, \rho_m(x)}{3.55}. \tag{5*}$$

The catalase distributions shown were derived by converting r in Eq. 2 to $c(r)$ on the basis of the data shown in Fig. 2. W is the time integral of the squared angular velocity; it is expressed here in nanoseconds^{-1} but is in seconds^{-1} in Eq. 1.

---

* Due to a typographical error, the constant 1.23 in this equation is given as 1.251 by Poole et al. (30) in their Eq. h. The correct value was used in their calculations.
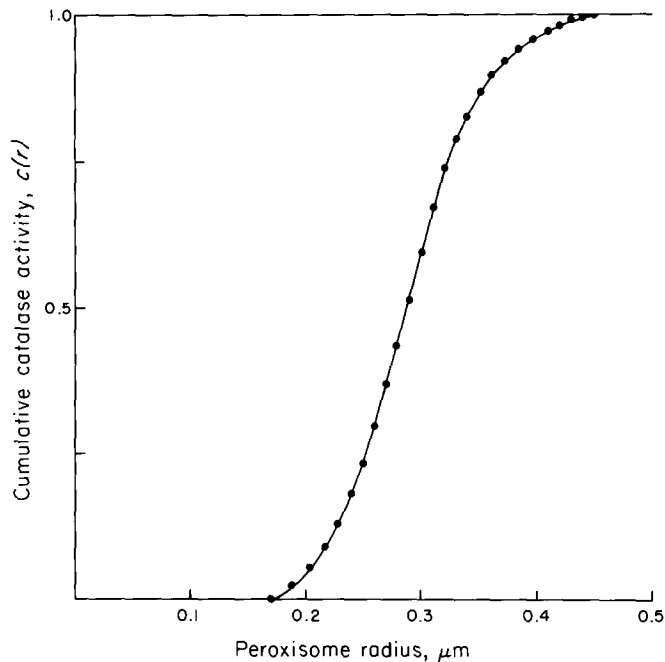
Figure 2 Cumulative size distribution of catalase. Circles are obtained from the size frequency distribution of catalase, as shown in Fig. 3 of Poole et al. (30), slightly truncated at either end. The fitted curve represents the following equations:

$$
\begin{aligned}
r < 0.174 \quad & c(r) = 0.0 \\
0.174 < r < 0.3136 \quad & c(r) = -0.5998 + 17.04\,r - 161.9\,r^2 + 602.6\,r^3 - 693.5\,r^4 \\
0.3136 < r < 0.434 \quad & c(r) = -11.12 + 87.72\,r - 225.4\,r^2 + 231.4\,r^3 - 67.96\,r^4 \\
r > 0.434 \quad & c(r) = 1.0
\end{aligned}
\tag{6}
$$

in which r is expressed in microns (it is in centimeters in Eq. 1).

distributions are broader than that predicted in Fig. 1, but this is due to the heterogeneity of the peroxisomes with respect to density, which was not taken into account in the computer-simulated experiment. As anticipated, the microsomal marker esterase, and even the ribosomal RNA, which tends to be associated with the denser microsomal subfractions (1, 45), are incompletely sedimented and have hardly entered the peroxisome-rich region of the gradient. Glucose-6-phosphatase, not shown on the graph, followed esterase very closely, as could be expected (1, 37). The mitochondria, which occupy a narrow band at density 1.18, indicated in Fig. 3 by a sharp protein peak and confirmed by cytochrome oxidase measurements, are clearly separated from the peroxisomes. They overlap with the microsomes, which, however, are distributed much more broadly.

Similar results can be obtained in the SW-39 swinging-bucket rotor, with 0.5 ml of PNS layered over a 4.6 ml linear gradient (1.10–1.27 density limits), itself resting on 0.3 ml of a 1.32 density cushion, centrifugation being performed with $W = 1.5 \times 10^{11}$ s^{-1}.

RESULTS

General Biochemical Results

In Fig. 4 are shown the averaged distributions observed for catalase, esterase, protein, and RNA. These distributions were very reproducible from one experiment to another, and the recoveries were satisfactory.

Fig. 5 illustrates the distributions found for TCA-precipitable radioactivity at various times after the injection of labeled leucine. At 3 min, the distribution of label follows approximately that of RNA. By 8 min the pattern has changed, becoming similar to that of the microsomal esterase, except for an unexplained excess of radioactivity in the fourth fraction from the top. Early labeling of the soluble proteins (top 2–3 fractions) also occurs. At later times, all that is seen is a slow shift of radioactivity from the microsomal to the soluble fractions, while the label associated with mitochondrial proteins begins to emerge as a peak
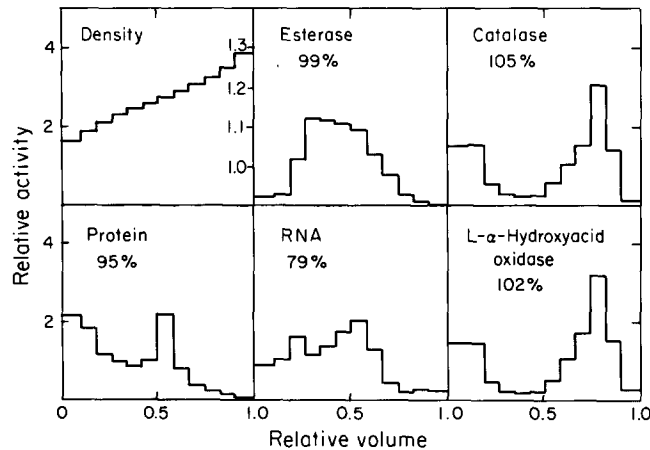
FIGURE 3 Distributions of biochemical markers after density gradient fractionation of PNS with $W = 1.4 \times 10^{10}$ s^{-1}. Percentage values refer to recoveries in gradient fractions.
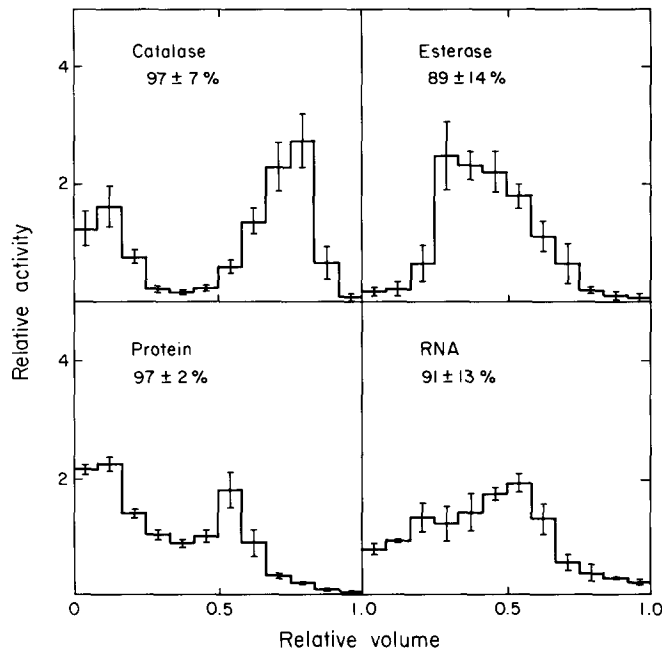

FIGURE 4 Averaged distributions of biochemical markers observed in 12 density gradient fractionations (three for RNA). Means ± standard deviation. Percentage values refer to recoveries in gradient fractions.

(fraction 6 from the bottom). It must be remembered that during the period between 10 and 60 min little new incorporation as well as little loss of label is seen (22). The observed shift of radioactivity could reflect synthesis of some cytosol proteins by microsome-bound ribosomes, or the passage of some labeled proteins into the plasma since the livers were not perfused.

The distribution of TCA-precipitable radioactivity from [^{3}H]ALA (Fig. 6) shows an initial mitochondrial peak, in agreement with the fact that the last enzyme in heme synthesis, ferrochelatase, is mitochondrial (25, 26, 36). With time there is a redistribution of label toward microsomes, probably reflecting the incorporation of new heme into cytochromes b_5 and P 450. The
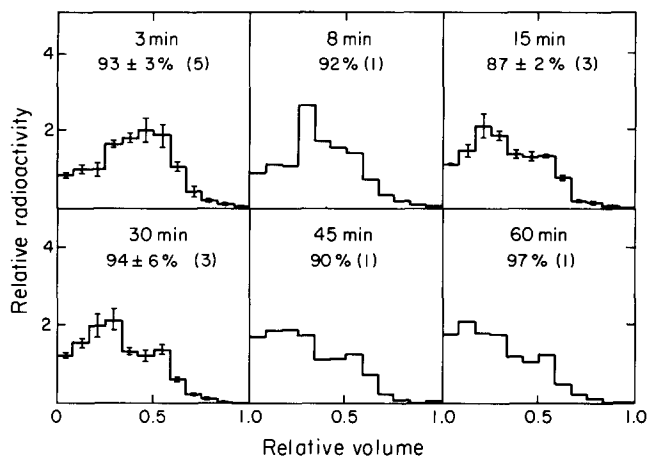
FIGURE 5 Distributions of TCA-precipitable radioactivities from labeled leucine at various times after injection of precursor. Means ± standard deviation. Between parentheses, number of experiments. Percentage values refer to recoveries in gradient fractions.
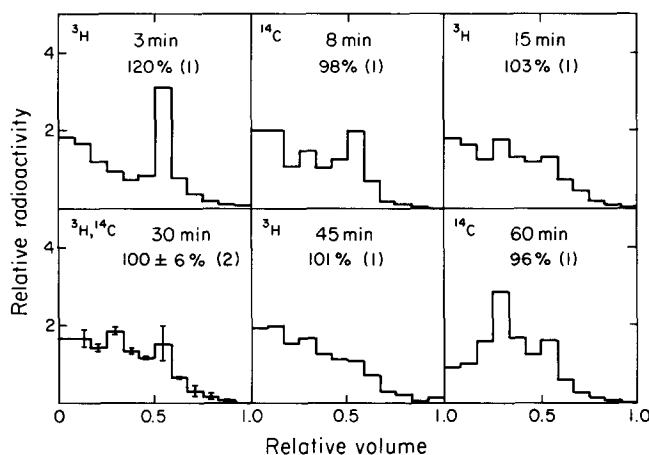

FIGURE 6 Distributions of TCA-precipitable radioactivities from labeled ALA at various times after injection of precursor. Means ± standard deviation. Between parentheses, number of experiments. Percentage values refer to recoveries in gradient fractions. The ALA was labeled with ^{3}H or ^{14}C as indicated.

distributions observed after injection of [^{14}C]ALA show the same trend. As pointed out in the preceding paper (22), they are not directly comparable on a kinetic basis with those obtained with [^{3}H]ALA, because the chemical dosages were much greater.

Distribution of Immunoprecipitable Radioactivity

Rats were double labeled with [^{3}H]leucine and [^{14}C]ALA, at the dosages shown in Table I, and sacrificed 8, 15, 30, and 60 min after labeling. General incorporation kinetics for these animals

have been reported in the preceding paper (22). As indicated in Table I, their weights and hepatic levels of marker enzymes were closely comparable. So were the enzyme distributions and recoveries after density gradient fractionation, which are included in Fig. 4. Recoveries of immunoprecipitable radioactivities are listed in Table II.

Table III shows the extent of the corrections that were made for nonspecific radioactivity in the immunoprecipitates from the gradient fractions. These were determined with control goat globulins as described previously (22). The corrections were generally small, indicating that our

TABLE I

Characteristics of Double-Labeled Rats

| Time | Body weight | Liver | | | |
		Weight	Protein	Catalase	Esterase
min	*g*	*g*	*mg/g*	*U/g*	*U/g*
8	220	9.0	162	52	147
15	250	8.1	180	57	173
30	235	7.8	185	53	163
60	240	8.8	195	56	153

TABLE II

Recoveries of Immunoprecipitable Radioactivities in the Gradients

| Time | WFI | | PCI | |
	[³H]leucine	[¹⁴C]ALA	[³H]leucine	[¹⁴C]ALA
min	*%*	*%*	*%*	*%*
15	98	50	84	60
30	111	66	111	77
60	130	99	86	86

Recoveries were not determined at 8 min.

immunoprecipitation technique could be reliably applied to the gradient fractions.

The corrected distributions of immunoprecipitable radioactivity are shown in Figs. 7 and 8. The leucine graphs were normalized to the same total surface area for the WFI, since we know from the kinetic data reported in the preceding paper (22) that leucine incorporation into the WFI is more than 95% completed at 8 min, and therefore that differences in leucine incorporation between the animals must be due mostly to individual variability. The surface area of the ALA graphs is proportional to the total amount of label incorporated.

Remembering that the peroxisomes band in the lower part of the gradient with a peak in the third fraction from the bottom, we see immediately from Fig. 7 that the actual incorporation of leucine into catalase does not take place in the peroxisomes themselves. We see further that the newly synthesized protein is quickly transferred to peroxisomes, and that this transfer occurs largely, if not totally, in the form of nonpurifiable intermediates. As early as 15 min after injection of the precursor amino acid, a substantial fraction of the total label is already found in the peroxisome region, mainly in nonpurifiable form. As time progresses,

TABLE III

Reliability of the Immunoprecipitation Technique as Applied to the Gradient Fractions (WFI)

| Time | Radioactivity in control precipitate, as percentage of radioactivity in immunoprecipitate* | |
	From [³H]leucine	From [¹⁴C]ALA
min		
8	50 ± 20	37 ± 11
15	13 ± 8	16 ± 8
30	28 ± 8	19 ± 12
60	27 ± 12	14 ± 14

Means ± standard deviation.
* Since the distributions of nonspecific label in the gradients are quite flat, these means reflect both larger values in those parts of the gradient where there is little labeled antigen, as well as much smaller values where the labeled antigen is concentrated. Thus at 8 min the correction to the leucine values is 28 ± 7% in fractions 1–4 but 63 ± 12% elsewhere (see Fig. 7). Similarly at 60 min the correction to the ALA values is 5 ± 3% in fractions 1–3 and 8–11, but 31 ± 7% in the center of the gradient (see Fig. 8). Obviously, if there were no labeled catalase species in a fraction the nonspecific label would be 100%.

both the size of this peak and its relative content in purifiable labeled catalase increase.

With ALA as precursor (Fig. 8), incorporation is delayed as seen before (22), but as it becomes evident, much of the incorporated label seems to appear immediately in the peroxisome region, and a considerable proportion of it is purifiable.

The distribution of the leucine label that does not sediment down to the peroxisome region is peculiar, especially at early times. It spans the starting layer in a strange "descending staircase" fashion, penetrating deeply into the gradient itself. As time goes on, this shape changes progressively to the distribution pattern of catalase enzyme activity (see Fig. 4). After 60 min, the distribution profiles of labeled material precipitated by anticatalase, whether derived from whole fractions or after partial purification of the enzyme, and with either leucine or ALA as precursor, are almost indistinguishable from that of catalase activity. By that time, therefore, the newly made catalase and the bulk of its biosynthetic intermediates are distributed like preexisting catalase, with about two-thirds associated with the peroxisome-rich fractions, and the remainder with the starting layer. Purifiable im-

munoprecipitable label seems to adopt this kind of distribution right from the start.

The main features of Figs. 7 and 8 were seen also in earlier experiments performed with less refined immunochemical methods, and in experiments in which the animals were double labeled with ALA and leucine, but with the isotopes reversed. Therefore, the results described here
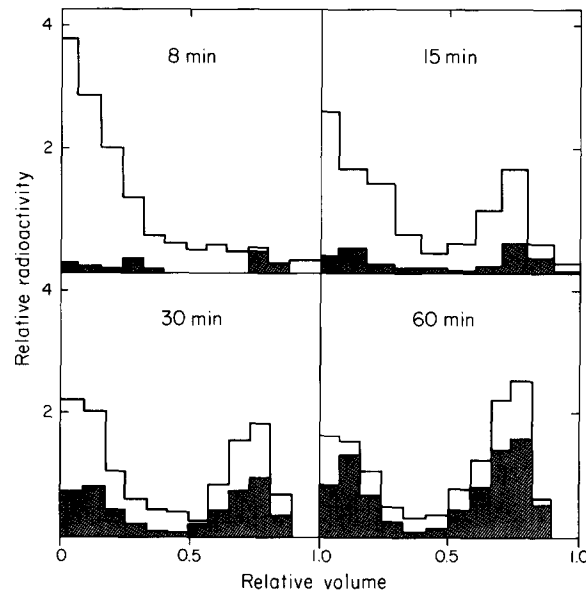

FIGURE 7 Distributions of immunoprecipitable radioactivities from [³H]leucine. Entire surface areas of diagrams represent radioactivities found in WFI, normalized to the same total surface area of 1. Cross-hatched parts are radioactivities of PCI. Difference between the two (white parts) represents radioactivity associated with nonpurifiable biosynthetic intermediates.
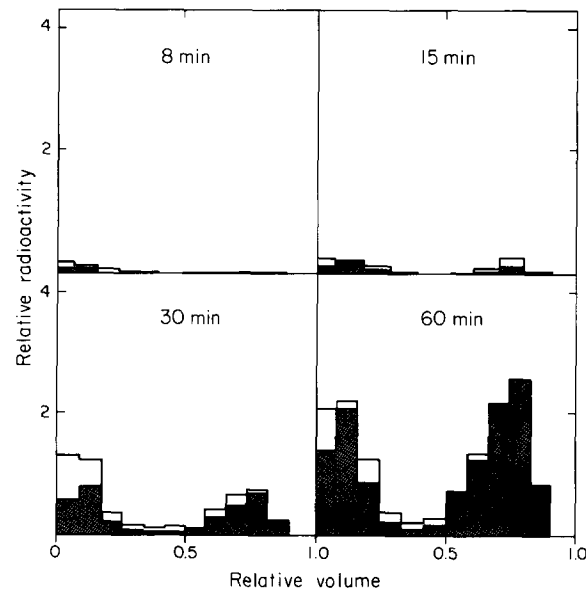

FIGURE 8 Distributions of immunoprecipitable radioactivities from [¹⁴C]ALA. Same representation as in Fig. 7, except that total surface areas of diagrams are proportional to incorporation, as shown in Fig. 7 of preceding paper (22).
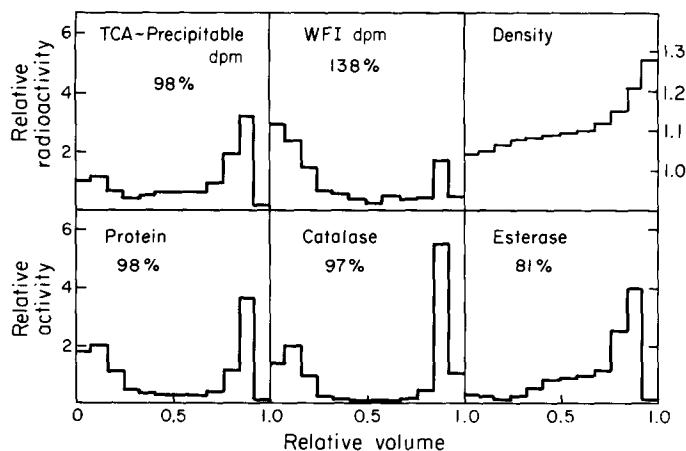
FIGURE 9 Distributions of markers and of TCA-precipitable and immunoprecipitable (WFI) radio-activities at 8 min after injection of 5 mCi of [³H]leucine. Regular gradient replaced by shallow gradient extending between densities 1.05 and 1.10.

may be taken as truly representative of the events of normal catalase biosynthesis.

In order to investigate the possibility that the descending staircase might reflect the equilibrium distribution of a polydisperse population of particles of low median density, a rat was labeled for 8 min with [³H]leucine, and the liver PNS was fractionated on a shallow gradient extending between density limits of 1.05 and 1.10. This gradient replaced the usual gradient, all other conditions being unchanged. The results are shown in Fig. 9. As could be predicted, mitochondria and peroxisomes have sedimented completely against the cushion, whereas microsomes are incompletely sedimented. Confirming the correlation shown in Fig. 5, TCA-precipitable radioactivity follows the microsomal esterase closely, except for some excess in the top fractions, also seen before. As to the immunoprecipitable radioactivity, it retains its characteristic descending staircase pattern, in spite of the considerable decrease in medium density and viscosity. Thus we cannot be dealing with low density particles. On the other hand, much of the radioactivity that is found in the body of the gradient under our standard conditions has moved down against the cushion. This part, therefore, is carried by particles, resembling microsomes in their sedimentation properties.

The possibility that the top rung of the descending staircase may reflect the partial flotation of the intermediate by virtue of an attachment to lipid was tested by boundary centrifugation of a postmicrosomal supernate from a rat labeled with

[³H]leucine for 8 min. At this time 89% of the label is in the first biosynthetic intermediate and only 9% in the second, as calculated from Eqs. 9, 10, and 12 in the preceding paper (22). As shown in Fig. 10 the label did not float; on the contrary it sedimented, but much more slowly than catalase itself. The sedimentation coefficient estimated from the midpoint of the boundary was 2.0S, corresponding to an $s'_{20,w}$ of 4.3S (7), in agreement with the values of 3.8-4.5S expected for a catalase subunit of molecular weight 60,000.[2] Furthermore, the sedimentation boundary of hemoglobin (mol wt 68,000), determined by visual inspection of the redness of the fractions, was in the same fraction as was that of the label. Therefore the first biosynthetic intermediate is a soluble aposubunit. Thus the descending staircase must be composed of several independent components. Part of the label is genuinely soluble. Part of it sediments, although slowly. The excess label seen in the top fraction is likely to be an artifact.

The kinetics with which immunoprecipitable label appears in soluble form in homogenates was examined in detail in rats given [³H]leucine by intraportal injection and killed at various times afterwards. Liver homogenates were prepared in the usual manner, and were then centrifuged for 2 h at 40,000 rpm. Pellet and supernate were assayed for marker enzymes and for total immuno-

---

[2] 3.8S was measured on formate-treated catalase in the presence of SDS (39). 4.5S was calculated from the $s^0_{20,w}$ of native tetrameric catalase (39) according to 4.5S = 11.3 S/4^{2/3}.

precipitable radioactivity. As seen in Fig. 11, label first appears in sedimentable form, and presumably represents nascent chains still bound to ribosomes. Immediately thereafter the label in the high-speed supernate rises rapidly, and by 5

min is equal to or greater than that in the sediment. With time there is a progressive redistribution of label until at 60 min two-thirds of the label are sedimentable (presumably in the intact peroxisomes), in agreement with the gradient results.

DISCUSSION

The Peroxisomal Pool

For a number of years, work from our laboratories has underscored the remarkable biochemical homogeneity of hepatic peroxisomes in female rats. If appropriate allowance is made for the presence of free cores bearing urate oxidase, all four peroxisomal markers, catalase, D-amino acid oxidase, L-α-hydroxyacid oxidase, and urate oxidase, show identical distributions in particulate preparations subfractionated on the basis of either density (3, 24) or sedimentation coefficient (30). About 70% of the activity of each enzyme can be accounted for in this way. The remainder is found either in soluble form (catalase, D-amino acid oxidase, L-α-hydroxyacid oxidase) or associated with free cores (urate oxidase), presumably arising from similarly homogeneous peroxisomes ruptured upon homogenization. The implication of these findings is that the distribution of catalase, as determined, for instance, in our gradient experiments, may be taken as representative of all other soluble peroxisomal components that do not significantly bind to sedimentable particles through adsorption artifacts. This point is illustrated by the similarity of the catalase and L-α-hydroxyacid oxidase distributions in Fig. 3.

In an earlier paper of this series, Poole et al. (30) have reported that newly made catalase is distributed between peroxisomes of different sizes
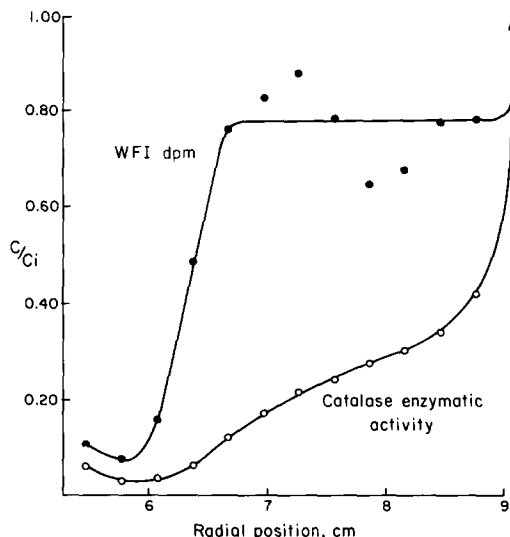

FIGURE 10 Sedimentation behavior of catalase and its biosynthetic intermediates. A high-speed supernate (38 min at 50,000 rpm, $W = 6.3 \times 10^{10}$ s^{-1}; 0.31 g liver/ml) was prepared from the liver of a rat labeled for 8 min with 5 mCi of [^{3}H]leucine. The supernate was centrifuged in an SW-39 rotor for 14 h at 39,000 rpm ($W = 8.4 \times 10^{11}$ s^{-1}), fractionated, and assayed for catalase enzymatic activity (O) and immunoprecipitable radioactivity, WFI ($\bullet$). The ordinate is the ratio of concentration C to average concentration C_i (sum of the activities of the fractions divided by total volume). For further experimental details and methods of computation of results, see reference 7.
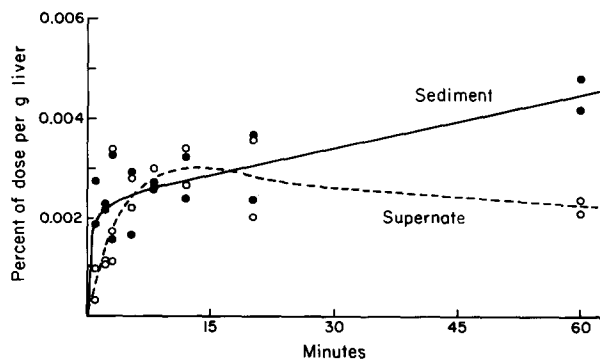

FIGURE 11 Kinetics of appearance of [^{3}H]leucine in immunoprecipitates (WFI) from high-speed supernate and sediment (2 h, 40,000 rpm). Dose was 1 mCi.

exactly like the soluble enzyme activities, as early as 3 h after injection of labeled leucine. They mention less complete observations indicating this to be true already 1 h after administration of the precursor. Our own results at 60 min agree entirely with these findings, and show in addition that the parallelism extends to the manner in which labeled material and enzymes are partitioned between the soluble and the particulate fractions. They make it highly probable that 1 h after injection of labeled leucine or ALA, both purifiable labeled catalase and its nonpurifiable biosynthetic intermediates are homogeneously distributed throughout the peroxisome population. Furthermore, they suggest that purifiable labeled catalase is distributed in this manner as soon as it appears.

We have tested the degree to which the above

conclusion is verified in individual experiments by the following calculation. Summing up the percentages of label and of catalase activity found in the four next to bottom gradient fractions, which contain a major part of the peroxisomes largely uncontaminated by other subcellular components, we first calculate the average ratio of immunoprecipitable radioactivity (total or purifiable) to catalase activity in intact peroxisomes for each experiment. Multiplying the catalase content of each fraction by this value, we then obtain the distribution that would be observed for the labeled catalase antigen, should it coincide with that of catalase. In Figs. 12 and 13 are shown the residual distributions remaining after subtraction of the distributions calculated in this manner. With leucine as precursor, this residue is negligible at all times for purifiable label, and it decreases with
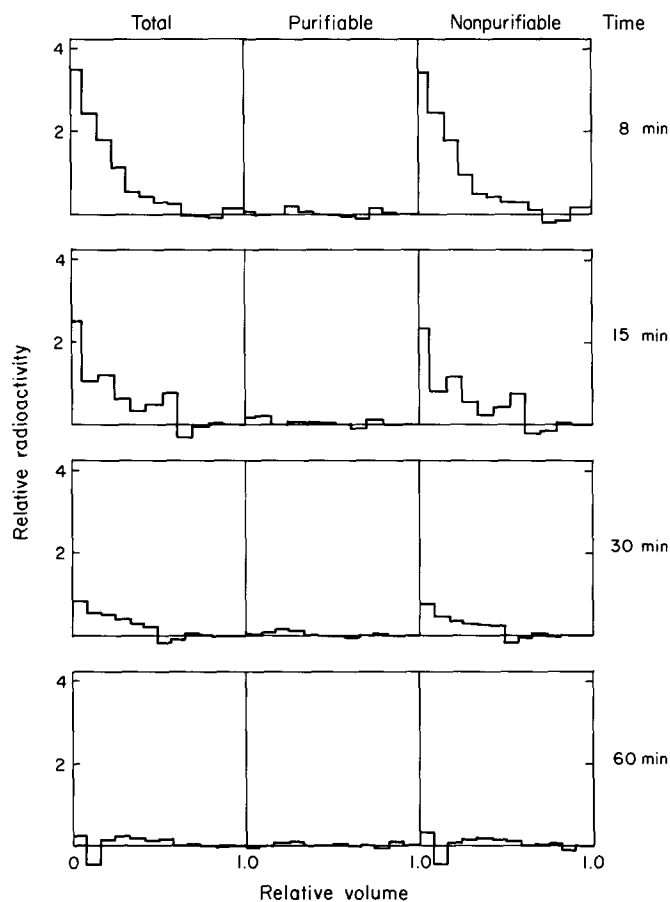

FIGURE 12   Distributions of nonperoxisomal immunoprecipitable radioactivities from [³H]leucine. These are the data of Fig. 7 after subtraction of peroxisomal label, assuming biochemical homogeneity, as described in the text. The three columns represent WFI, PCI, and the difference, WFI-PCI, respectively.

time to become practically negligible after 60 min for nonpurifiable label. With ALA as precursor, there is very little left at all times of either purifiable or nonpurifiable label. These facts provide strong additional evidence in support of the homogeneity hypothesis, and validate the use of the ratio of immunoprecipitable radioactivity to catalase activity in the peroxisome-rich gradient fractions as a measure of the proportion of immunoprecipitable label associated with peroxisomes in the intact cells (see below).

It would appear from the above considerations that the homogeneity of the peroxisomal pool is such as to cause newly made catalase to invade the whole pool uniformly almost immediately after entering it. One view compatible with such behavior (30) and with a number of morphological observations (11, 16, 28, 31, 35, 40, 41, 43) is that

which pictures many peroxisomes in a given cell as being interconnected with each other to form a single membrane-bounded space of homogeneous content. The alternative, also considered before (30), is that the newly synthesized catalase is confined to a small number of newly made particles that cannot be distinguished from the bulk of the peroxisome population on the basis of either size or density.

Kinetics of Transfer of Label to Peroxisomes

In Figs. 14 and 15 is shown the manner in which nonpurifiable and purifiable immunoprecipitable radioactivities are distributed between the extra- and intraperoxisomal compartments at various times after the intraportal injection of the labeled
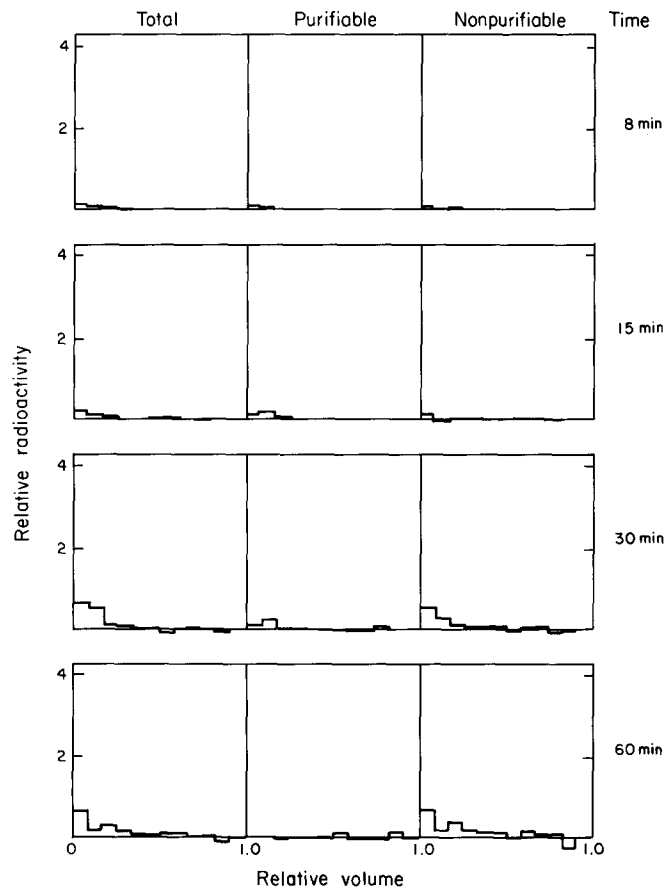

FIGURE 13 Distributions of nonperoxisomal immunoprecipitable radioactivities from [^{14}C]ALA. These are the data of Fig. 8 after subtraction of peroxisomal label, assuming biochemical homogeneity, as described in the text. The three columns represent WFI, PCI, and the difference, WFI-PCI, respectively.

precursors. The amounts associated with the peroxisomes were calculated on the basis of the homogeneity hypothesis as explained above. This is equivalent to taking the areas in Figs. 12 and 13 as measuring the amount of label present outside the peroxisomes.

The leucine data (Fig. 14) indicate that the protein part of catalase is synthesized outside the peroxisomes and is delivered into an extraperoxisomal pool of nonpurifiable intermediate, which empties rapidly into the peroxisomes where the catalase molecule is completed. There is a suggestion from the ALA results (Fig. 15) that some heme addition may occur outside the peroxisomes. But this possibility rests on small differences in radioactivity between the two precipitates (see Fig. 8), obtained in experiments where the kinetics of heme metabolism were seriously disturbed by the administration of large amounts of ALA. The rapid transfer of leucine-labeled intermediate to the peroxisomes (Fig. 14), together with what is known of the kinetics of the overall process of catalase biosynthesis (22), makes it likely that the
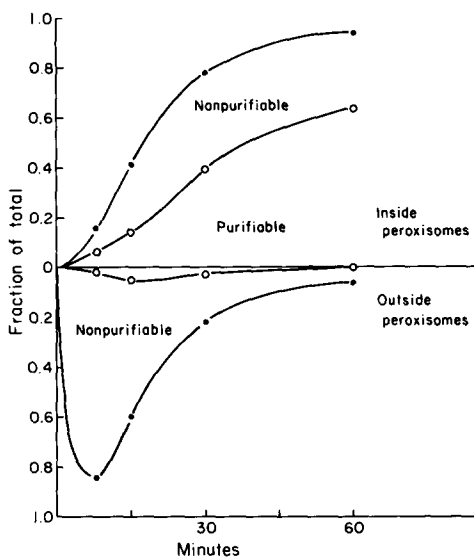

FIGURE 15 Subcellular compartmentation of biosynthetic intermediates with label from [^{14}C]ALA. Same representation as in Fig. 14 but based on the data of Figs. 8 and 13.

FIGURE 14 Subcellular compartmentation of biosynthetic intermediates labeled with [^{3}H]leucine. The upper half of the figure shows the WFI (●) and PCI (○) radioactivities in the peroxisomes, calculated from the data of Fig. 7, assuming biochemical homogeneity as described in the text. The lower half of the figure shows the nonperoxisomal label; the ordinate values equal the areas under the histograms of Fig. 12, left (●) and center (○) columns.
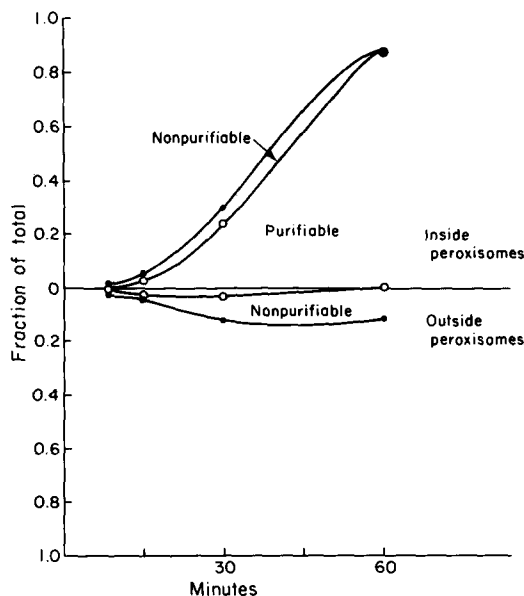
bulk of heme addition takes place inside the peroxisome.

To account for the above results, we must amend the kinetic model proposed in the preceding paper (22), by introducing in it two distinct pools of hemeless intermediate, one extra- and the other intraperoxisomal. The kinetics of filling and emptying of the extraperoxisomal pool are depicted clearly in Fig. 14, and the data are easily fitted to the system of equations examined previously (22). We find for the turnover time of the extraperoxisomal pool of intermediate a value of the order of 20 min, corresponding to a pool size of 0.65% of the total catalase or 5 μg/g liver.

Due to the disturbance introduced by the injection of large amounts of ALA, the results obtained with this precursor cannot be used for the purpose of kinetic analysis. But the results of Fig. 14 can be fitted to a simplified model assuming a single intraperoxisomal pool of intermediates, having a turnover time of the order of 25 min, corresponding to a pool size of 0.8% of the total catalase or 6.5 μg/g liver. Since at least two pools are involved, one of hemeless and the other of heme-containing intermediate, these estimates are upper limits. They suggest that in the present experiments, the total amount of non-

purifiable intermediates was of the order of 1.5% of the total catalase content or less. This estimate is lower than the value of 2.1% obtained in the preceding paper (22). As briefly commented upon in that paper, this difference, if significant, could be another aspect of the kinetic disturbance caused by ALA.

Site of Biosynthesis of Catalase

The theory that catalase is made by bound ribosomes has rested for more than 10 yr on the kinetic data of Higashi and Peters (15), which, except for an unexplained early peak in the supernatant fraction, appeared to illustrate the existence of a sequence leading from rough-surfaced microsomes to particles which the authors at that time called "mitochondria" and we now know to be peroxisomes. In the original paper, the results were plotted in the form of the specific radioactivities of the fractions. We have replotted them in Fig. 16 in terms of disintegrations per minute per milligram liver, calculated from the specific radioactivities and the catalase antigen distribution data given by the authors (14).

This representation brings to light two important features of the results of Higashi and Peters (15) that were not clearly apparent in their original publication. It shows first that the early peak in the supernatant fraction is in fact quite substantial, in agreement with the results reported here and with those of Redman et al. (33). It reveals further that almost 40% of the labeled
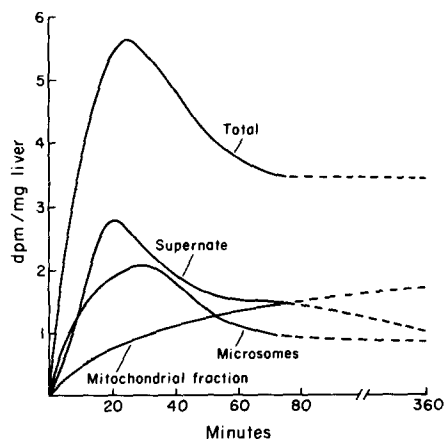

FIGURE 16 Data of Higashi and Peters (15) replotted as disintegrations per minute per milligram liver. Calculated from the specific radioactivities and the catalase antigen distribution data given by the authors (14).

material precipitated by anticatalase disappeared from the liver between the 20th and 60th min after injection of the precursor leucine. Partial intracellular destruction of an unstable intermediate could conceivably account for this phenomenon, which, however, was observed neither by Redman et al. (33) nor by us (22). A more likely explanation is that the early immunoprecipitates contained a highly labeled contaminant. This could be a protein of very high turnover, or, more probably, a secretory protein such as serum albumin, which is known to be discharged some 20 min after its formation (12, 29, 33). Indeed, the authors mention that their antisera "gave a few weak lines against undiluted rat serum" but that they removed the contaminating antibodies by adsorption with "a slight excess of combined α_2 and γ-globulin fraction" (14). Whatever the explanation, we feel that the disappearance of a significant portion of the label throws some doubt on the significance of the early labeling of a rough microsomal fraction observed by Higashi and Peters (15). Since all authors agree on the high degree of labeling of the supernatant fraction, the material lost from the liver more likely originated from the microsomes (see Fig. 16), which happens to be the fraction in which the newly synthesized plasma proteins would be found.

The presence of a contaminant in the catalase immunoprecipitates isolated from rough microsomes has in fact been reported by Higashi and Peters (14), who found in such precipitates 2.3 times more apparent antigen than there was enzymatically active catalase in the fraction. The authors suggest that the enzymatically inactive antigen might be a precursor of the enzyme. But this is very unlikely. As shown in this paper, the nonperoxisomal enzyme precursor is largely in the supernatant fraction. Furthermore, the microsomal material detected by Higashi and Peters (14) amounts to as much as 90 μg/g liver, more than 5 times the total amount made up by the two biosynthetic intermediates, and almost 20 times the amount present in the extraperoxisomal pool, according to our estimates.

In more recent publications, Higashi and coworkers (13, 19) have reported the immunochemical precipitation of ribosome-bound nascent catalase from preparations of both bound and free polysomes. They conclude that both types of ribosomes participate in the synthesis of catalase, but that the membrane-bound ribosomes play the major role. Here again, however, the crucial ques-

tion of specificity must be raised since the authors recover as much as 5% of the total liver ribosomes by their immunoprecipitation technique. This contrasts with the fact that catalase synthesis represents only 0.5% of the total protein synthesizing activity of the liver (22).

Other workers who have tried to identify the site of catalase synthesis have had little or no success. Takagi et al. (42) have obtained some evidence of in vitro synthesis of catalase by both free and bound polysomes, but the observed levels of incorporation were very low and the authors do not consider their results conclusive. Redman et al. (33) have attempted to detect nascent chains after puromycin release, but they obtained negative results with both free and bound polysomes.

Our own efforts to look for nascent catalase chains after either in vivo or in vitro labeling have been similarly unsuccessful. We did obtain labeled immunoprecipitates from both bound and free ribosomes treated with puromycin, but in our experience, puromycin-released chains, especially those from free polysomes (see also reference 32), have very high levels of nonspecific precipitation, and the adequacy of immunoprecipitation for quantitative analysis of nascent chains of minor proteins is not clear. The variety of physical properties to be found in a population of growing chains precludes any simple physico-chemical tests of immunochemical specificity. For the moment we feel that there is no adequate direct evidence as to whether free or bound polysomes or both synthesize catalase.

Mode of Transfer of Catalase to Peroxisomes

We find that the newly synthesized catalase antigen appears rapidly in the supernatant fraction. The data of Higashi and Peters are compatible with this (see Fig. 16) and Redman et al. (33) have recently published similar results. Our results demonstrate further that the labeled material at that stage consists of aposubunits of about 60,000 molecular weight. The distribution of this material in the gradient does not parallel that of the soluble proteins, but rather shows a characteristic descending staircase pattern. The peak in the top fraction is probably an artifact but the penetration of part of the label into the gradient region occupied by the microsomes requires an explanation. It could conceivably be due to an adsorption artifact, or it could reflect the specific association of labeled material with small particles. Arguing in favor of the second explanation is the fact that the amount of label found in the microsomal region of the gradient does not decrease together with the amount present in soluble form.

The simplest interpretation of our results is that catalase is synthesized by free polysomes, which could well be concentrated in the third, fourth, and fifth fractions from the top, thereby accounting for the lower part of the staircase. The newly synthesized catalase would be released directly into the cell sap, explaining the rapid appearance of soluble labeled antigen.

However, we cannot exclude other possibilities. Catalase could be synthesized by bound ribosomes, but delivered into the cytosol rather than into the cisternal lumen, as suggested by Legg and Wood (23). Or it could be made by both free and bound ribosomes, as proposed by Higashi and co-workers (13, 19). Or it could be synthesized in, or rapidly transferred to, a fragile cytoplasmic particle, which is largely destroyed by homogenization. Such a particle could account for the lower part of the staircase. Functionally, it could serve as a vehicle in the transport of the newly made catalase to the peroxisomes. Or it could even be a peroxisome precursor, the elusive growth form searched for unsuccessfully in earlier experiments (30). The identification of such a structure by biochemical isolation is probably hopeless, because it would constitute only a very small fraction of the microsomes. A cytochemical identification seems equally improbable, since the modified 3,3'-diaminobenzidine (DAB) staining reaction for catalase (27), being dependent on a peroxidatic activity, is unlikely to give a positive result with a hemeless precursor of the enzyme. For this reason, we are inclined to attribute to experimental artifact the staining patterns that have led Legg and Wood (23) to suggest that catalase is made by ribosomes attached to the ER, but is delivered on the cytosol side of the ER membranes, where it subsequently diffuses into adjacent peroxisomes through the membrane of these particles.

Conclusion

According to the "classical" theory of peroxisome biogenesis, these particles arise as budding outgrowths of the smooth ER; their enzymes are believed to be synthesized by bound ribosomes,
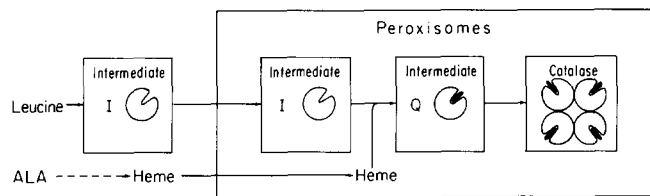
FIGURE 17 Summarized topology of catalase biosynthesis. The representation of intermediate Q as a subunit is hypothetical.

discharged intracisternally as they are made, and conveyed into the growing peroxisomes through ER channels. This theory, in addition to borrowing some concepts from findings made on very different systems (5, 17, 18, 34, 38), has rested mainly on morphological observations of widespread connections between peroxisomes and the ER (11, 16, 28, 31, 35, 40, 41, 43) and on the biochemical results of Higashi and Peters (15), as they were interpreted by de Duve and Baudhuin (8) to fit newly acquired knowledge on the structural and functional properties of peroxisomes. The results described in the present paper provide no support to this theory and all earlier attempts made in this laboratory to verify some of its implications have been unsuccessful.

Our results taken at their face value suggest that the newly made apomonomer of catalase is discharged mainly into the cytosol, appears partly, either simultaneously or perhaps subsequently, in a small particulate component, and is then finally transferred to peroxisomes where heme addition and completion of the catalase molecule take place (Fig. 17). One could visualize the small particulate component either as a vehicle for the transfer of the protein to the peroxisomes or as a precursor transforming into a new peroxisome. In either case, the process must be such as to lead to a distribution pattern indistinguishable from that of preexisting peroxisomal enzymes. The whole process is very rapid, with a half-time for appearance of labeled intermediates in the peroxisomes of about 14 min. As we have seen, except for a possible difference of opinion concerning the site of catalase biosynthesis, all published biochemical data would be in substantial agreement with a view of this sort.

We should not, however, disregard the morphological evidence for attachment of peroxisomes to the ER, nor accept too lightly the possibility that a protein of molecular weight 60,000 could be taken up selectively from the cytosol into a

membrane-bounded structure. There is, of course, an alternative interpretation to our results that is consistent with the classical theory. If peroxisomes form some sort of continuum, directly connected with a specialized subset of ER involved in the synthesis and transport of their constituents, fragmentation of this structure by homogenization could cause a greater release of contents from the ER and connecting elements than from the peroxisomes themselves. Realizing this possibility, we have made a number of attempts, using the gentlest possible homogenization procedures, to obtain a hint of the existence of such fragile elements, so far unsuccessfully.

REFERENCES

1. AMAR-COSTESEC, A., H. BEAUFAY, E. FEYTMANS, D. THINES-SEMPOUX, and J. BERTHET. 1969. Subfractionation of rat liver microsomes. *In* Microsomes and Drug Oxidations. J. R. Gillette, A. H. Conney, G. J. Cosmides, R. W. Estabrook, J. R. Fouts, G. J. Mannering, editors. Academic Press, Inc., New York. 41.
2. BAUDHUIN, P., H. BEAUFAY, Y. RAHMAN-LI, O. Z. SELLINGER, R. WATTIAUX, P. JACQUES, and C. DE DUVE. 1964. Tissue fractionation studies. 17. Intracellular distribution of monoamine oxidase, aspartate aminotransferase, alanine aminotransferase, D-amino acid oxidase and catalase in rat liver tissue. *Biochem. J.* 92:179.
3. BEAUFAY, H., P. JACQUES, P. BAUDHUIN, O. Z. SELLINGER, J. BERTHET, and C. DE DUVE. 1964. Tissue fractionation studies. 18. Resolution of mitochondrial fractions from rat liver into

three distinct populations of cytoplasmic particles by means of density equilibration in various gradients. *Biochem. J.* **92**:184.

4. BLOBEL, G., and V. R. POTTER. 1968. Distribution of radioactivity between the acid-soluble pool and the pools of RNA in the nuclear, nonsedimentable and ribosome fractions of rat liver after a single injection of labeled orotic acid. *Biochim. Biophys. Acta.* **166**:48.

5. CARO, L. G., and G. E. PALADE. 1964. Protein synthesis, storage, and discharge in the pancreatic exocrine cell. An autoradiographic study. *J. Cell Biol.* **20**:473.

6. CHANCE, B. 1950. The reactions of catalase in the presence of the notatin system. *Biochem. J.* **46**:387.

7. DE DUVE, C. 1972. Is there a glycolytic particle? *In* Structure and Function of Oxidation Reduction Enzymes. Å. Åkeson and A. Ehrenberg, editors. Pergamon Press Inc., New York. 715.

8. DE DUVE, C., and P. BAUDHUIN. 1966. Peroxisomes (microbodies and related particles). *Physiol. Rev.* **46**:323.

9. DE DUVE, C., J. BERTHET, and H. BEAUFAY. 1959. Gradient centrifugation of cell particles: theory and applications. *Prog. Biophys. Biophys. Chem.* **9**:325.

10. DE DUVE, C., B. C. PRESSMAN, R. GIANETTO, R. WATTIAUX, and F. APPELMANS. 1955. Tissue fractionation studies. 6. Intracellular distribution patterns of enzymes in rat-liver tissue. *Biochem. J.* **60**:604.

11. ESSNER, E. 1967. Endoplasmic reticulum and the origin of microbodies in fetal mouse liver. *Lab. Invest.* **17**:71.

12. GLAUMANN, H. 1970. Studies on the synthesis and transport of albumin in microsomal subfractions from rat liver. *Biochim. Biophys. Acta.* **224**:206.

13. HIGASHI, T., H. KUDO, and K. KASHIWAGI. 1972. Specific precipitation of catalase-synthesizing ribosomes by anticatalase anti-serum. *J. Biochem. (Tokyo).* **71**:463.

14. HIGASHI, T., and T. PETERS, JR. 1963. Studies on rat liver catalase. I. Combined immunochemical and enzymatic determination of catalase in liver cell fractions. *J. Biol. Chem.* **238**:3945.

15. HIGASHI, T., and T. PETERS, JR. 1963. Studies on rat liver catalase. II. Incorporation of ¹⁴C-leucine into catalase of liver cell fractions *in vivo*. *J. Biol. Chem.* **238**:3952.

16. HRUBAN, A., H. SWIFT, and R. W. WISSLER. 1963. Alterations in the fine structure of hepatocytes produced by β-3-thienylalanine. *J. Ultrastruct. Res.* **8**:236.

17. JAMIESON, J. D., and G. E. PALADE. 1967. Intracellular transport of secretory proteins in the pancreatic exocrine cell. I. Role of the periph-

eral elements of the Golgi complex. *J. Cell Biol.* **34**:577.

18. JAMIESON, J. D., and G. E. PALADE. 1967. Intracellular transport of secretory proteins in the pancreatic exocrine cell. II. Transport to condensing vacuoles and zymogen granules. *J. Cell Biol.* **34**:597.

19. KASHIWAGI, K., T. TOBE, and T. HIGASHI. 1971. Studies on rat liver catalase. V. Incorporation of ¹⁴C-leucine into catalase by isolated rat liver ribosomes. *J. Biochem.* **70**:785.

20. LAZAROW, P. B. 1971. Biosynthesis of peroxisome catalase in rat liver. Proceedings of the 11th Annual Meeting of The American Society for Cell Biology. 161.

21. LAZAROW, P. B. 1972. The biogenesis of peroxisomal catalase in rat liver. Ph.D. Thesis. The Rockefeller University, New York.

22. LAZAROW, P. B., and C. DE DUVE. 1973. The synthesis and turnover of rat liver peroxisomes. IV. Biochemical pathway of catalase synthesis. *J. Cell Biol.* **59**:491.

23. LEGG, P. G., and R. L. WOOD. 1970. New observations on microbodies. A cytochemical study on CPIB-treated rat liver. *J. Cell Biol.* **45**:118.

24. LEIGHTON, F., B. POOLE, H. BEAUFAY, P. BAUDHUIN, J. W. COFFEY, S. FOWLER, and C. DE DUVE. 1968. The large-scale separation of peroxisomes, mitochondria, and lysosomes from the livers of rats injected with Triton WR-1339. *J. Cell Biol.* **37**:482.

25. MINAKAMI, S., Y. YONEYAMA, and H. YOSHIKAWA. 1958. On the biosynthesis of heme and hemeproteins in liver cell. *Biochim. Biophys. Acta.* **28**:447.

26. NISHIDA, G., and R. F. LABBE. 1959. Heme biosynthesis. On the incorporation of iron into protoporphyrin. *Biochim. Biophys. Acta.* **31**:519.

27. NOVIKOFF, A. B., and S. GOLDFISCHER. 1969. Visualization of peroxisomes (microbodies) and mitochondria with diaminobenzidine. *J. Histochem. Cytochem.* **17**:675.

28. NOVIKOFF, A. B., and W. Y. SHIN. 1964. The endoplasmic reticulum in the Golgi zone and its relations to microbodies, Golgi apparatus and autophagic vacuoles in rat liver cells. *J. Microsc. (Paris).* **3**:187.

29. PETERS, T., JR. 1962. The biosynthesis of rat serum albumin. II. Intracellular phenomena in the secretion of newly formed albumin. *J. Biol. Chem.* **237**:1186.

30. POOLE, B., T. HIGASHI, and C. DE DUVE. 1970. The synthesis and turnover of rat liver peroxisomes. III. The size distribution of peroxisomes and the incorporation of new catalase. *J. Cell Biol.* **45**:408.

31. REDDY, J., and D. SVOBODA. 1971. Microbodies

in experimentally altered cells. VIII. Continuities between microbodies and their possible biologic significance. *Lab. Invest.* 24:74.

32. REDMAN, C. M. 1969. Biosynthesis of serum proteins and ferritin by free and attached ribosomes of rat liver. *J. Biol. Chem.* 244:4308.

33. REDMAN, C. M., D. J. GRAB, and R. IRUKULLA. 1972. The intracellular pathway of newly formed rat liver catalase. *Arch. Biochem. Biophys.* 152:496.

34. REDMAN, C. M., P. SIEKEVITZ, and G. E. PALADE. 1966. Synthesis and transfer of amylase in pigeon pancreatic microsomes. *J. Biol. Chem.* 241:1150.

35. RHODIN, J. A. G. 1963. An Atlas of Ultrastructure. W. B. Saunders Company, Philadelphia.

36. SANO, S., and S. GRANICK. 1961. Mitochondrial coproporphyrinogen oxidase and protoporphyrin formation. *J. Biol. Chem.* 236:1173.

37. SHIBKO, S., and A. L. TAPPEL. 1964. Distribution of esterases in rat liver. *Arch. Biochem. Biophys.* 106:259.

38. SIEKEVITZ, P., and G. E. PALADE. 1960. A cytochemical study on the pancreas of the guinea pig. V. *In vivo* incorporation of leucine-1-C^{14} into the chymotrypsinogen of various cell fractions. *J. Biophys. Biochem. Cytol.* 7:619.

39. SUND, H., K. WEBER, and E. MÖLBERT. 1967. Dissoziation der Rinderleber-Katalase in ihre Untereinheiten. *Eur. J. Biochem.* 1:400.

40. SVOBODA, D. J., and D. L. AZARNOFF. 1966. Response of hepatic microbodies to a hypolipidemic agent, ethyl chlorophenoxyisobutyrate (CPIB). *J. Cell Biol.* 30:442.

41. SVOBODA, D., H. GRADY, and D. AZARNOFF. 1967. Microbodies in experimentally altered cells. *J. Cell Biol.* 35:127.

42. TAKAGI, M., T. TANAKA, and K. OGATA. 1970. Functional differences in protein synthesis between free and bound polysomes of rat liver. *Biochim. Biophys. Acta.* 217:148.

43. TSUKADA, H., Y. MOCHIZUKI, and T. KONISHI. 1968. Morphogenesis and development of microbodies of hepatocytes of rat during pre- and postnatal growth. *J. Cell Biol.* 37:231.

44. WEISSMANN, B. 1969. A colorimetric method for α-naphthol and its application to assay of hydrolases. *Anal. Biochem.* 28:295.

45. WIBO, M., A. AMAR-COSTESEC, J. BERTHET, and H. BEAUFAY. 1971. Electron microscope examination of subcellular fractions. III. Quantitative analysis of the microsomal fraction isolated from rat liver. *J. Cell Biol.* 51:52.